CO_2 geological storage: Microstructure and mechanical behavior of cement modified with a biopolymer after carbonation

Juan Cruz Barría[1,2], *Diego* Manzanal[3,*], *Jean-Michel* Pereira[2], and *Siavash* Ghabezloo[2]

[1]Engineering Faculty, Universidad Nacional de la Patagonia San Juan Bosco, 9004 Comodoro Rivadavia, Chubut, Argentina.
[2] Navier, Ecole des Ponts, Univ Gustave Eiffel, CNRS, Marne-la-Vallée, France.
[3]E.T.S.I. Caminos, Universidad Politécnica de Madrid, Prof. Aranguren 3, 28040 Madrid, Spain.

Abstract. Large amounts of CO_2 could be stored underground in deep rock reservoirs and could help reducing emissions into the environment. Carbon geo-storage technologies have several years in development and new techniques and materials are being studied to make this procedure more effective and less expensive. The risk of leakage from geological reservoirs to other rock formations or even towards the surface means that long-term behavior must be carefully studied. The carbonation of the cement used for sealing the wellbore may compromise the borehole integrity. In light of this problem, this work aims to analyze the poromechanical behavior of cement with and without a new additive in a CO_2 environment. Bacterial nanocellulose is a biopolymer that modifies important cement properties such as compressive strength, thermal behavior and hydration degree. Two cement types were studied: class G cement and modified class G cement with bacterial nanocellulose. These samples were submitted to a supercritical CO_2 environment (temperatures higher than 32 °C and pressures higher than 8 MPa) during 30 days. Mercury intrusion porosimetry and uniaxial compressive strength tests were performed on these samples to study the effect of carbonation. Both types of cement are affected after carbonation by reducing compressive strength and Young's modulus (E), however, the strength of modified cement was reduced by 8%, while non-modified cement was reduced by 20%.

1 Introduction

Pollution has increased considerably over the last 100 years, mainly in the most developed countries nowadays. Even though these developed countries have been trying to decrease their CO_2 pollution, global CO_2 emissions are increasing at a significant rate [1].

The decrease of CO_2 sources and their replacement by renewable energy is the next step to stop dependency on fossil fuels and the pollution they produce. At the same time, one way to prevent CO_2 from reaching the atmosphere is the CO_2 geological storage. By capturing the CO_2 from power or cement plants, we are able to inject it underground in deep reservoirs. Particularly, we can take advantage of the performed works for oil extraction. Once the well ceases to be productive, the CO_2 can be injected through the same pipes.

A thin annular layer of cement separates the casing from the reservoir, whose purpose is to prevent leakage paths to other rock formations. Initially, cement can withstand static downhole conditions. However, long-term integrity must be carefully studied.

The carbonation process starts when cement is placed in an acidic CO_2 medium. After CO_2 is injected, its concentration will depend on pressure and temperature. At temperatures and pressures higher than 32°C and 8 MPa, the CO_2 is in a supercritical state, thus having a density like that of a liquid and the viscosity of a gas. These conditions may increase the chemical reactions in the carbonation process.

Leaching in cement begins with the chemical reactions between the calcium hydroxide (CH) and carbon dioxide (CO_2). The ions saturation in the fluid makes precipitate calcium carbonate (CC) in pores. At the same time, H_2O is released and fluid pressure is increased. The pH level is decreased by the loss of CH and may enhance the hydrated calcium silicate (CSH) leaching and casing corrosion.

$$CH + CO_2 \rightarrow CC + H_2O \quad (1)$$

The mechanical performance is modified by the leaching of CSH, which may compromise the long-term wellbore integrity.

$$0.625CSH + CO_2 \rightarrow CC + 1.3H_2O + 0.625SiO_2(H_2O)_{0.5} \quad (2)$$

Bacterial nanocellulose is a biopolymer derivate from the bacteria *Gluconatetobacter Xylinus* with high mechanical properties such as high Young's modulus and high tensile strength [2].

Recent studies have found that nanocellulose increases the hydration degree and mechanical properties of cement [3-4], which may improve cement performance by inhibiting its cracking and preventing degradation due to carbonation. However, it is necessary to carry out experiments and to analyze the behavior of the cement in

* Corresponding author: d.manzanal@upm.es

order to characterize the effects produced by the nanocellulose.

The objective of this work is to study the poromechanical properties of modified cement samples with bacterial nanocellulose by performing mercury intrusion porosimetry (MIP) and uniaxial compressive strength (UCS) tests. The study focuses on modified cement behavior after carbonation in a CO_2 geological storage context, and compares its behavior to that of standard Portland Cement.

2 Experimental characterization

2.1. Materials

Cement was provided by Petroquímica Comodoro Rivadavia S.R.L. and two different mixtures were prepared: an API Class G Portland Cement (CEM I) with high sulfate resistance grade (HSR) as a reference, whose composition is described in [5], and the same cement with the addition of nanocellulose (BNC).

The biopolymer used was bacterial nanocellulose gel with approximately 98% of water and 2% of bacterial nanocellulose. It was provided by Nanocellu-Ar, a spinoff of the Institute of Polymer Technology and Nanotechnology (ITPN) of Buenos Aires and it comes in the form of a membrane gel. It was obtained from the fermentation of the bacteria *Gluconatetobacter Xylinus*, which produces fibers having a diameter between 20 and 40 nm and a length of 1 μm [6].

2.2. Methods

2.2.1 Sample preparation

To obtain a higher degree of homogenization, the polymer was crushed using a blender and then placed in an ultrasound device. We added 0.15% of bacterial nanocellulose by weight of cement for the modified cement. This addition increases considerably the yield stress of the slurry [7]. A superplasticizer was used in this case to reduce its viscosity and maintain a fluid mixture similar to CEM I. Both mixtures had a water to cement ratio of 0.44.

The samples were prepared according to the API standard 10A[8], the slurry was then poured into cylindrical molds of 38 mm of diameter by 76 mm high and they were cured under alkaline water for 28 days.

2.2.2 Supercritical carbonation

Samples were weighed, measured and placed inside a titanium cell. After sealing the cell, it was connected to the CO_2 line pressure and filled (5 MPa approximately). The pump was turned on and we continued to inject CO_2 up to 8MPa. Once this pressure was reached, we increased the temperature to 90 °C inside the cell. The increase in temperature causes the CO_2 pressure to rise, so the pressure was controlled by the relief valve until it reached 20 MPa. Both temperature and pressure were measured and controlled during the entire experiment.

Carbonation was performed at 90 °C and 20 MPa for 30 days. After that, the heating was turned down and the pressure was slowly diminished for 1 hour until atmospheric pressure was reached. Samples were weighed and photographed.

2.2.3 Porosimetry

Mercury intrusion porosimetry (MIP) tests were performed on non-carbonated and carbonated samples. The samples were taken from the external surface for carbonated cement. First, they were dried by freeze-drying method and then kept in plastic jars half full silica gel until testing. Pore size distribution can be obtained by force equilibrium of the meniscus between liquid mercury and its vapor by Laplace equation:

$$D = \frac{4 * \gamma * cos(\theta)}{P} \quad (3)$$

in which: D is the pore access diameter, ϒ is the mercury surface tension, θ is the contact angle between the liquid and the solid surface and P is the applied pressure.

2.2.4 Uniaxial compressive strength

Samples were tested on a universal testing machine with a maximum load of 100 kN at a speed of 0.5 mm/min. The values were calculated by taking the average of 3 tested cylindrical samples. Maximum compressive strength and Young's modulus were obtained. The axial displacement is given by the machine readings, so calibration was made in order to avoid misreadings.

3 Results

Carbonation depends essentially on the curing conditions for cement since several experiences from different authors have shown diversity on results for similar cement types [5-6]. Fig. 1 shows a change in color on the surface after carbonation. This change in color is likely to be amorphous precipitation of iron hydroxides or magnesium iron aluminum hydrates from the hydrated calcium aluminate phase (AFm) [11], [12]. However by cutting radially in the center of the samples, we observe a slow penetration rate (Fig. 2), due to a high hydration degree at this cement age [13].

The area most degraded by the color change is observed only in the zone near the exposed surface. Here, a maximum carbonation penetration depth of 3.5 mm for CEM I and 1.5 mm for BNC is measured. The preferential carbonation path is observed around the pores near the surface, as shows the Fig. 3. The measured depth takes into account this effect. However, if we want to be independent of this particularity, the carbonation front of CEM I would be at 2.5 mm and 1.0 mm for BNC. Nevertheless, more up-to-date studies show that chemical reactions penetrate further into the sample [14].

Fig. 1. Samples before and after carbonation

Fig. 2. Radial cut on samples after carbonation (CEM I and BNC)

The age and type of curing of the cement allow it to be fully hydrated and the porosity to be very small compared with porosities obtained by other authors in cement types class G or H [15]. The previous laboratory studies [7-8] have shown that BNC increases hydration components even more after 28 days of curing, mainly due to the hydrophilic capacity of BNC which allows maintaining water inside the mixture for prolonged times, enabling more complete chemical reactions to take place. Bacterial nanocellulose fibers are highly resistant [2] and during hydration, they might reduce cracks caused during drying. This improvement could reduce larger pores and slow down the penetration rate into the cement during setting and then in the hardened cement stage [16]. The depth of penetration of CO_2 into the interior of the cement depends mainly on permeability and diffusion, which in turn are estimated in theory by the porosity of the sample [17].

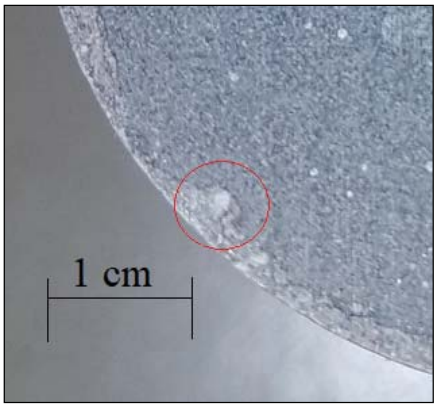

Fig. 3. Carbonation depth of CEM I.

Initial bulk density was determined: 1.99 kg/cm^3 for CEM I and 1.97 kg/cm^3 for BNC. After carbonation, density was increased until 2.02 and 2.00 kg/cm^3 respectively, with a mass uptake of 2.7 g for CEM I and 2.1 g for BNC. The mass increment is due to the precipitation of CC, which is denser than CH.

The cumulative mercury intrusion is shown in Fig. 4. MIP performed on non-carbonated samples reveals a porosity decrease from CEM I (19%) to BNC (13%). The characteristic peak is moved from 50 nm to 45 nm (Fig. 5). These results are linked with our penetration rate results shown before. Bacterial nanocellulose in BNC samples are reducing porosity and pore size diameter at some point while curing the cement. By reducing larger pores, the transport parameters are modified and they may tend to reduce the CO_2 transfer towards the center of cement samples.

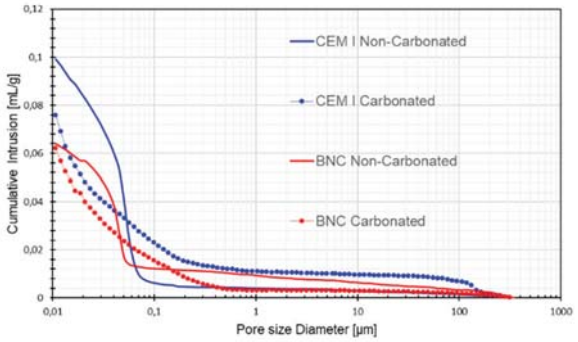

Fig. 4. Cumulative mercury intrusion

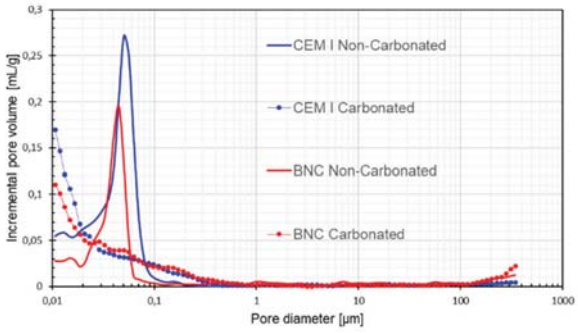

Fig. 5. Incremental pore volume

After carbonation, samples taken from the zone near the exposed surface suffers a porosity variation due to CC precipitation in pores; porosity is decreased on CEM I to 15% and to 12% on BNC. The peaks at 45 and 50 nm disappear but smaller pores start to appear as we can see in Fig 4. We can also observe a small increment in larger pores of 200 nm. The disappearance of the peak at 45 and 50 nm is the result of CC growing inside the pores. During the chemical reactions, one mole of CH is replaced by one mole of CC. As the molar volume and density of CC are higher than CH, cement pores begin to fill up with CC and bulk density of samples is increased. The increment in pores of 200 nm results from damage during or after carbonation in the process of pressure release[18]. Another possible cause could be the continued growth of

CC inside the pores until clogging and this may damage the pore surface with tensile stress, generating bigger cracks[19]. As depletion, carbonation and degradation fronts are microscopic layers [12], [20] and the MIP takes macroscopic samples of 1 cm^3 approximately, the difference between them cannot be made. Thus, the MIP tests in the present work is more influence by the CC barrier, which blocks the inwards access. Nevertheless, the MIP curves suggest that the entire sample contains CC, supporting the initial idea that the dissolution and carbonation fronts have penetrated more into the interior of the sample than seen by the brown color change of the edges.

Before carbonation, both types of cement have similar strength: 55 MPa for BNC and 53 MPa for CEM I. This small variation might be the effect of the bacterial nanocellulose, which by enhancing the hydration kinetics, may generate more nuclei to promote the degree of hydration, thus allowing cement to be more resistant [21]. Young's modulus has been measured and both types of cements gave approximately 26 GPa.

After 30 days of carbonation, CEM I loses 20% of its initial strength while BNC loses 8% (Fig. 6). Adding a reinforcement of bacterial nanocellulose increases cement tensile stress, therefore, also preventing cement to be affected as CEM I and maintaining its compressive strength during carbonation. There has been a wide variation in results in some author's experiences [9, 17, 18] depending on temperature and pressure imposed during the carbonation stage. Nevertheless, there is no agreement yet on the mechanical results after carbonation.

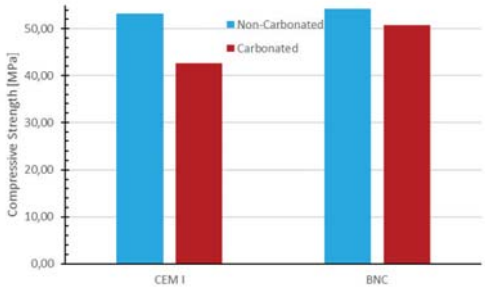

Fig. 6. Cement strength after carbonation

Most of previous authors' experiences have short curing times for the cement. At the time of carbonation, their cement may not be fully hydrated and the mechanical performance increment after carbonation might be due to the hydration acceleration imposed by temperature in the carbonation cell. Their tested material might be in fact a combination of hydration cement compounds and calcite that has been reacting with CH during the hydration in the cell. In our case, our cement is relatively highly more hydrated and chemically stable after being cured 28 days in alkaline water. The only possible effect of CO_2 is to react with CH and no hydration reaction will be in progress, this is why we can observe a decrease in compressive strength and in Young's Modulus, which is observed in both cements after carbonation, and giving a similar value (Fig. 7). It decreased by 14% for CEM I and 17% for BNC.

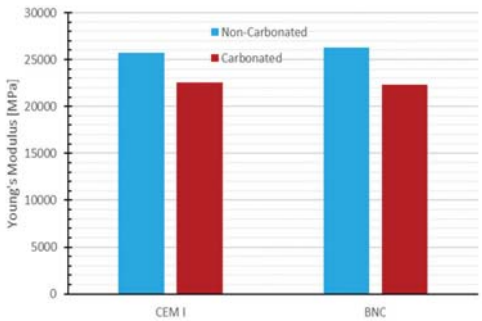

Fig. 7. Young's modulus on carbonated samples

Density and Young's modulus are larger for CC than for CH, i.e. CC precipitation should increase mechanical performance. However, CSH might be losing its integrity by being dissolved while CC is precipitating, but CC is not being bounded to the cement matrix as CSH was initially. This may create a discontinuity which diminishes the mechanical properties. This behavior is pointed out in [23], wherein the calcite precipitation zone, Young's modulus is lower than in the unreacted zone. If carbonation continues, Young's modulus will continuously decrease until reaching the silica gel Young's modulus [23].

Given the lower compressive strength and Young's modulus, results on BNC carbonated samples consistently show a variation on axial strain (Fig. 8). This strain change was also noted in CEM I and on similar tests that we have performed. Ductility is changing in time; this behavior will be studied on further works analyzing the volumetric changes during carbonation.

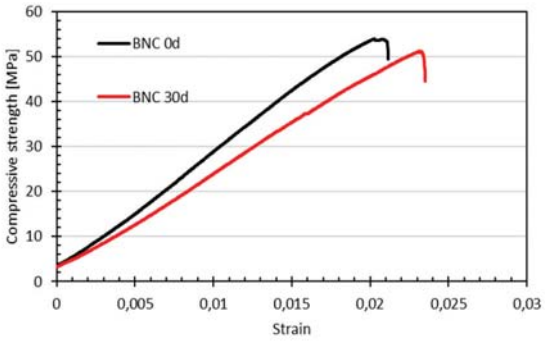

Fig. 8. Carbonation effect on compressive strength.

4 Conclusions

This work studies the accelerated carbonation of class G oil well cement modified samples with a bio-polymer, product of the synthesis of the Gluconatetobacter Xylinus bacteria called bacterial nanocellulose.

The result of the process of immersing the samples in supercritical CO_2 at a pressure of 20 MPa and a temperature of 90 °C for 30 days seeks to emulate the conditions to which the cement sheath is subjected in the depleted oil wells used in the geological storage of CO_2.

The study evaluates the microstructural changes of cement and modified cement samples before and after

carbonation with a mercury porosimeter. In addition, mechanical behavior is characterized with uniaxial tests.

Before carbonation, the addition of bacterial nanocellulose reduces porosity by 30% compared to portland cement porosity of 19%. The additive also reduces the characteristic peak of the pore size diameter from 50 nm (CEM I) to 45 nm (BNC). Uniaxial compressive strength is 4% higher on the modified cement and Young's modulus is the same in both cases.

After the carbonation process, non-modified cement shows penetration of 2.5 mm while penetration depth is 40% lower in cement with bacterial nanocellulose, probably due to the initial porosity decrease compared to portland cement.

The density of the samples increases by 1.5% for both types of cement. Porosity is decreased but CEM I shows a higher variation. Pore size distribution is changed, the characteristic peak is moved to 10 nm and some small cracks are generated during carbonation at 200 nm. Cement maximum strength is diminished but BNC has lower strength loss than CEM I and Young's modulus is reduced as well.

The addition of bacterial nanocellulose is increasing the poromechanical performance of cement before carbonation by reducing its initial porosity and increasing compressive strength. Its effect is also maintained after carbonation by slowing down the penetration rate of CO_2, diminishing porosity which reduces the transport parameter inside cement, and by keeping compressive strength below a 10% variation from its initial value.

Further works will be focused on higher carbonation times, allowing more penetration depth and analyzing the compounds and mechanical performance variation through time.

Acknowledgments

The first author gratefully acknowledges the technical staff of the NAVIER laboratoire for helping with the performed tests and to the EIFFEL fellowship program of Excellence granted by the Ministre de l'Europe et des Affaires étrangères of France.

References

1. J. M. Belbute and A. M. Pereira, "*ARFIMA Reference Forecasts for Worldwide CO2 Emissions and the Need for Large and Frontloaded Decarbonization Policies,*" Lisboa, (2019).
2. P. Gatenholm and D. Klemm, "*Bacterial Nanocellulose as a Reneable Material for Biomedical Applications,*" *MRS Bull.*, vol. **35**, pp. 208–213, (2010), doi: 10.1080/15440478.2018.1439426.
3. O. A. Hisseine, W. Wilson, L. Sorelli, B. Tolnai, and A. Tagnit-Hamou, "*Nanocellulose for improved concrete performance: A macro-to-micro investigation for disclosing the effects of cellulose filaments on strength of cement systems,*" *Constr. Build. Mater.*, vol. **206**, pp. 84–96, (2019), doi: 10.1016/j.conbuildmat.2019.02.042.
4. X. Sun, Q. Wu, S. Lee, Y. Qing, and Y. Wu, "*Cellulose Nanofibers as a Modifier for Rheology, Curing and Mechanical Performance of Oil Well Cement,*" *Sci. Rep.*, vol. **6**, pp. 1–9, (2016), doi: 10.1038/srep31654.
5. J. C. Barría, A. Vazquez, P. Cerrutti, and D. Manzanal, "*Effect of Bacterial Nanocellulose on class G cement,*" (2020).
6. P. Cerrutti, P. Roldán, R. M. García, M. A. Galvagno, A. Vázquez, and M. L. Foresti, "*Production of bacterial nanocellulose from wine industry residues: Importance of fermentation time on pellicle characteristics,*" *J. Appl. Polym. Sci.*, vol. **133**, no. 14, (2016), doi: 10.1002/app.43109.
7. C. G. Hoyos, R. Zuluaga, P. Gañán, T. M. Pique, and A. Vazquez, "*Cellulose nanofibrils extracted from fique fibers as bio-based cement additive,*" *J. Clean. Prod.*, vol. **235**, pp. 1540–1548, (2019), doi: 10.1016/j.jclepro.2019.06.292.
8. API Specification 10A, *Specification for Cements and Materials for Well Cementing*. 2010.
9. V. Barlet-Gouedard, G. Rimmelé, B. Goffé, and O. Porcherie, "*Well Technologies for CO 2 Geological Storage : CO 2 -Resistant Cement,*" *SPE Int.*, vol. **62**, no. 3, pp. 325–334, (2007), doi: 10.2516/ogst.
10. B. G. Kutchko, B. R. Strazisar, G. V. Lowry, D. a. Dzombak, and N. Thaulow, "*Rate of CO2 Attack on Hydrated Class H Well Cement under Geologic Sequestration Conditions,*" *Environ. Sci. \& Technol.*, vol. **42**, no. 16, pp. 6237–6242, (2008), doi: 10.1021/es800049r.
11. S. H. Yin, Y. F. Yang, T. S. Zhang, G. F. Guo, and F. Yu, "*Effect of carbonic acid water on the degradation of Portland cement paste: Corrosion process and kinetics,*" *Constr. Build. Mater.*, vol. **91**, pp. 39–46, (2015), doi: 10.1016/j.conbuildmat.2015.05.046.
12. Y. J. Jeong, K. S. Youm, and T. S. Yun, "*Effect of nano-silica and curing conditions on the reaction rate of class G well cement exposed to geological CO2-sequestration conditions,*" *Cem. Concr. Res.*, vol. **109**, no. September 2017, pp. 208–216, (2018), doi: 10.1016/j.cemconres.2018.05.001.
13. J. C. Barria, D. Manzanal, C. M. Martín, T. M. Pique, and J. M. Pereira, "*Cement-rock interface subjected to scCO2,*" in *14th International Congress Rock Mechanics and Geotechnical Engineering*, 2019, pp. 3196–3203.
14. J. C. Barría, D. Manzanal, J.-M. Pereira, and S. Ghabezloo, "*Study on poromechanical changes of nanocellulose cement composite subjected to supercritical CO2,*" (2020).

15. J. C. Barría, D. Manzanal, and J. M. Pereira, "*CO2 Geological Storage: Performance of Cement-Rock Interface,*" in *Proceedings of the XVI Pan-American Conference on Soil Mechanics and Geotechnical Engineering (XVI PCSMGE)*, 2019, pp. 2873–2881, doi: 10.3233/STAL190359.
16. M. Panchuk, L. Shlapak, A. Panchuk, M. Szkodo, and W. Kiełczy, "*Perspectives of use of nanocellulose in oil and gas industry,*" *J. Hydrocarb. Power Eng.*, vol. **3**, no. 2, pp. 79–84, (2016).
17. S. Ghabezloo, J. Sulem, and J. Saint-Marc, "*Evaluation of a permeability-porosity relationship in a low-permeability creeping material using a single transient test,*" *Int. J. Rock Mech. Min. Sci.*, vol. **46**, no. 4, pp. 761–768, (2009), doi: 10.1016/j.ijrmms.2008.10.003.
18. A. Fabbri *et al.*, "*Effect of carbonation on the hydro-mechanical properties of Portland cements,*" *Cem. Concr. Res.*, vol. **39**, no. 12, pp. 1156–1163, (2009), doi: 10.1016/j.cemconres.2009.07.028.
19. D. Manzanal, V. Vallin, and J. M. Pereira, "*A chemo-poromechanical model for well/caprock interface in presence of CO2,*" *Poromechanics V - Proc. 5th Biot Conf. Poromechanics*, pp. 1470–1477, (2013), doi: 10.1061/9780784412992.175.
20. B. G. Kutchko, B. R. Strazisar, D. A. Dzombak, G. V. Lowry, and N. Thauiow, "*Degradation of well cement by CO2 under geologic sequestration conditions,*" *Environ. Sci. Technol.*, vol. **41**, no. 13, pp. 4787–4792, (2007), doi: 10.1021/es062828c.
21. T. Fu, R. J. Moon, P. Zavattieri, J. Youngblood, and W. J. Weiss, *Cellulose nanomaterials as additives for cementitious materials*, vol. **C**. Elsevier Ltd, 2017.
22. A. Fabbri *et al.*, "*Effect of carbonation on the hydro-mechanical properties of Portland cements,*" *Cem. Concr. Res.*, vol. **39**, no. 12, pp. 1156–1163, (2009), doi: 10.1016/j.cemconres.2009.07.028.
23. H. E. Mason, W. L. Du Frane, S. D. C. Walsh, Z. Dai, S. Charnvanichborikarn, and S. A. Carroll, "*Chemical and Mechanical Properties of Wellbore Cement Altered by CO 2 - Rich Brine Using a Multianalytical Approach,*" *Environ. Sci. Technol.*, vol. **47**, pp. 1745–1752, (2013), doi: dx.doi.org/10.1021/es3039906.